Water weakening of clinopyroxene in the dislocation creep regime

S. Chen,[1] T. Hiraga,[1] and D. L. Kohlstedt[1]

Received 14 June 2005; revised 16 March 2006; accepted 14 April 2006; published 17 August 2006.

[1] We performed a series of triaxial compressive creep experiments at two different water fugacities to investigate the effect of water on the creep strength of a natural clinopyroxenite. Samples were deformed under water-saturated conditions at temperatures between 1373 and 1473 K, confining pressures of 150 and 300 MPa, and differential stresses from 34 to 261 MPa. Strain rates were in the range 10^{-7} to 10^{-5} s^{-1}. Water fugacity was controlled at either 140 or 280 MPa. The creep results yield a stress exponent of 2.7 ± 0.3 and an activation energy of 670 ± 40 kJ/mol. Compared to dry clinopyroxene, wet samples creep over 100 times faster at a given temperature, confining pressure, water fugacity, and differential stress. The creep rate of clinopyroxene is proportional to the water fugacity to the 3.0 ± 0.6 power, with an activation volume of 0 m^3/mol. One possible water-weakening mechanism is an enhancement of the rate of dislocation climb associated with increases in the concentration of jogs and the diffusivity of silicon ions. Compared to other major minerals in Earth's lower crust, specifically olivine and plagioclase, the water-weakening effect is most significant for clinopyroxene. Under hydrous conditions the strengths of clinopyroxene and anorthite are comparable over the investigated stress range, and both phases are weaker than olivine. Since the mineral assemblages in Earth's lower continental crust are often dominated by plagioclase and pyroxene, in places where a wet flow law applies, the mechanical behavior of clinopyroxene will have a substantial effect on creep strength.

Citation: Chen, S., T. Hiraga, and D. L. Kohlstedt (2006), Water weakening of clinopyroxene in the dislocation creep regime, *J. Geophys. Res.*, *111*, B08203, doi:10.1029/2005JB003885.

1. Introduction

[2] Clinopyroxene (cpx) is a major constituent of the lower crust. It is found in a wide range of geological environments, such as metamorphic, shear, and continental cratonic zones. Studies on water content in nominally anhydrous minerals have shown that pyroxene is the most "hydrous", holding up to 75000 H/10^6Si in natural and synthesized samples [*Skogby et al.*, 1990; *Smyth et al.*, 1991; *Bell and Rossman*, 1992; *Katayama and Nakashima*, 2003]. Since only a trace amount of water is needed to enhance the rate of dislocation as well as diffusion creep, with the abundance and high water solubility of cpx, the mechanical properties of clinopyroxene aggregates under hydrous conditions may exert a significant influence on the creep strength of Earth's continental lithosphere in localities where a wet creep condition applies.

[3] The creep behavior of dry clinopyroxene aggregates has been studied by several researchers. *Bystricky and Mackwell* [2001] reported results from a series of deformation experiments on dry Sleaford Bay clinopyroxenite in both the dislocation and the diffusion creep regimes at a range of P-*T* conditions. They deformed both cored (coarse-grained) and hot-pressed (fine-grained) samples. *Dimanov et al.* [2003] also investigated the creep strength of fine-grained synthesized diopside; in this case, samples were fabricated by melting binary oxides under dry conditions. However, knowledge of the mechanical behavior of wet clinopyroxene remains limited. The first report on the water-weakening effect on clinopyroxene in dislocation creep was made by *Boland and Tullis* [1986]. They performed constant strain rate experiments on Sleaford Bay clinopyroxenite with 0.5–1.0 wt% H_2O added at 300 MPa from 1463 to 1543 K and showed that the clinopyroxene aggregates were weaker under hydrous conditions than under anhydrous conditions. *Hier-Majumder et al.* [2005] determined the diffusion creep strength of fine-grained samples fabricated from Sleaford Bay clinopyroxenite under both hydrous and anhydrous conditions. In these experiments, water-saturated aggregates crept about 30 times faster than dry ones. The water-weakening effect for clinopyroxene is larger than that for olivine [*Mei and Kohlstedt*, 2000a] and anorthite in the diffusion creep regime [*Rybacki and Dresen*, 2000].

[4] As a continuation of the exploration on the mechanical properties of wet clinopyroxenes, we have performed a series of dislocation creep tests on Sleaford Bay clinopyroxenite under water-saturated conditions. The goal of this research is to determine the dependence of the dislocation creep rate on water fugacity as well as the possible mech-

[1]Department of Geology and Geophysics, University of Minnesota, Minneapolis, Minnesota, USA.

0148-0227/06/2005JB003885$09.00

anism of water weakening. The results of this study provide important information for better understanding the strength of Earth's lower continental crust.

2. Experimental Details

2.1. Sample Assembly Preparation

[5] The samples used in this study were natural clinopyroxenites from the Precambrian metamorphic terrain of Sleaford Bay, South Australia. On the basis of electron microprobe analyses, the chemical composition of this material is $Ca_{0.98}Mg_{0.79}Fe_{0.256}Al_{0.017}Na_{0.012}Si_2O_6$ with about 1% opaque impurity phases [*Boland and Tullis*, 1986]. The average grain size, determined from optical micrographs using the line intercept method with a correction factor of 1.5 [*Gifkins*, 1970] is 530 ± 20 μm; this value is similar to that reported by *Bystricky and Mackwell* [2001] on material from the same locality if the factor of 1.5 is also applied to their measurement. Cylinders were cored with a length-to-diameter ratio of more than 2:1, and the ends were ground flat and parallel. The lengths and diameters of cylinders for wet deformation experiments were 17.9 to 18.3 mm and 7.0 to 7.2 mm, and the length and diameter of the sample for the dry deformation test were 18.4 and 8.9 mm, respectively. For the dry deformation experiment, the sample was annealed in a one-atmosphere furnace at 1273 K for 10 hours with the oxygen fugacity controlled near the Ni/NiO phase boundary using mixed CO/CO_2 gases.

[6] Experiments were performed under both hydrous and anhydrous conditions. For anhydrous conditions a sample was placed into a thin wall (0.2 mm thick) nickel capsule made from two single-end, telescoping cans. The capsule sealed along the interface between the inner can and the outer can when pressure was applied. For experiments conducted under hydrous conditions a sample was placed into a thin wall Ni sleeve (50 μm thick), then slid into a talc sleeve with Ni rings at either end (1.2 mm thick), and finally put into telescoping Ni cans, as illustrated in Figure 1. Since the chemical composition of talc changes with time as it dehydrates, its strength gradually increases. The nickel rings added at the top and bottom of the talc sleeve circumvent this complication because nickel, which is much weaker than talc, controls the rate of deformation of this portion of the sample assembly. Therefore, in correcting the values measured for load to obtain the load (stress) on the sample, we only need to consider the load supported by the iron jacket plus the nickel capsule and rings. Because the telescoping cans seal when pressure is applied, water is kept inside the capsule during a deformation experiment at high-temperature, high-pressure conditions.

[7] Near 1075 K at a confining pressure of 300 MPa, talc decomposes into water and enstatite to yield 4.5 wt% water. The presence of water and enstatite provide both a hydrous environment and a silica buffer. Oxygen fugacity and water fugacity were buffered by the Ni/NiO solid-state reaction with the fluid pressure equate to the confining pressure. Different water fugacities were achieved by changing the confining pressure.

2.2. Deformation Experiments

[8] To prepare for an experiment, the encapsulated sample along with zirconia and alumina pistons were inserted into an iron jacket [*Mei and Kohlstedt*, 2000a]. The sample assembly was heated in a gas medium, mechanical testing apparatus [*Paterson*, 1990]. Temperature was controlled and monitored by using a R-type (Pt-Pt 13% Rh) thermocouple. On the basis of temperature calibrations of the furnace, temperature varies by less than 2 K along the sample length. Constant load compressive deformation experiments were performed at temperatures between 1373 and 1473 K, confining pressures of 150 and 300 MPa, and differential stresses from 34 to 261 MPa. Measured strain rates ranged from 10^{-7} to 10^{-5} s^{-1}. Some samples were deformed at multiple temperatures and multiple differential stresses to determine the activation energy and stress exponent for creep under hydrous conditions.

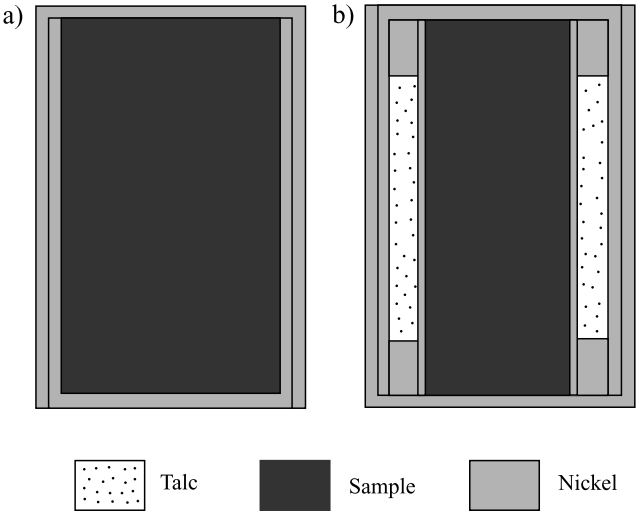

Figure 1. Sketch of sample assemblies used for deformation experiments carried out under (a) anhydrous conditions and (b) hydrous conditions. Drawing is not to scale.

[9] For every deformed sample, creep data were obtained by varying the stress at constant temperature and pressure. The differential stress was calculated from the load divided by the area of the sample; the reported values are accurate to within ±2 MPa. The strain rate was calculated from the displacement versus time data, which were obtained by varying the stress step by step at constant temperature and confining pressure. Stress and strain rate data were corrected (1) for the load supported by the iron jacket and nickel capsule using flow laws for Fe and Ni reported by *Frost and Ashby* [1982] and (2) for the change in sample area and length during deformation. After deformation, the samples were cooled to room temperature at a rate of 100 K/min and 50 MPa/min without load.

[10] For experiments conducted under hydrous conditions, the sample assemblies were pierced to check for the presence of water after the experiments. All the samples were cut into sections for microstructural and water concentration analyses.

2.3. Infrared Analysis

[11] The concentration of water in samples deformed under either dry or wet conditions was measured using transmitted infrared (IR) radiation in the microscope attachment of a Nicolet Fourier transform infrared (FTIR) spec-

Table 1. Experimental Conditions for Deformation of Clinopyroxene Aggregates[a]

	Experiment	Dry/Wet	T, K	P, MPa	ε_{total}, %
PI-1125	deformation	dry	1473	300	4
PI-1196	deformation	wet	1473	300	10
PI-1197	deformation	wet	1473	300	10
PI-1209	deformation	wet	1473	300	12
PI-1211	deformation	wet	1473	150	8
PI-1215	deformation	wet	1473	150	7
PI-1216	deformation	wet	1473	300	9
PI-1219	deformation	wet	1448	150	4
PI-1224	deformation	wet	1373–1448	300	13

[a] T is temperature, P is pressure, and ε_{total} is total strain.

trometer. A thin slice was cut from each cylindrical sample and polished to a thickness of <200 μm for FTIR analysis. Four to eight spectra in the wave number range 500 to 4000 cm^{-1} were collected for each sample on clean spots inside of single grains under a stream of dry air. A 100 μm aperture was used, and 256 scans were accumulated for each spectrum. Each spectrum was corrected for baseline using a spline fit obtained from regions on either side and the bases of the peaks. Then the hydroxyl (OH) content of the samples was calculated on the basis of the calibration by *Paterson* [1982],

$$C_{OH} = \frac{X_i}{150\gamma} \int \frac{K(\overline{\upsilon})}{3780 - \overline{\upsilon}} d\overline{\upsilon} \tag{1a}$$

and the calibration by *Bell et al.* [1995],

$$C_{OH} = \frac{1}{I_{\|}\gamma} \int K(\overline{\upsilon}) d\overline{\upsilon} \tag{1b}$$

where C_{OH} is the hydroxyl concentration, and X_i, the density factor, depends on chemical composition. For clinopyroxene, $X_i = 6.7 \times 10^4$ H/10^6Si. $I_{\|}$ is the integral extinction coefficient given by 1.16 cm^{-2} per H/10^6 Si. The orientation factor, γ, is given by 1/3 for an unpolarized beam, and $K(\overline{\upsilon})$ (in cm^{-1}) is the absorption coefficient at wave number $\overline{\upsilon}$ (in cm^{-1}).

2.4. Chemical Analysis

[12] The chemical composition of Sleaford Bay clinopyroxene was obtained using an electron probe microanalyzer. Analyses were carried out at 15 kV and 10 nA with a 10 s peak counting time and a 5 s background time. Nineteen randomly chosen spots on the sample were analyzed, and the major element compositions were calculated from the average.

2.5. Microstructural Analysis

[13] The microstructures of both the starting material and the deformed samples were analyzed with a transmitted light optical microscope. Dislocation structures of samples deformed under dry and wet conditions were analyzed using transmission electron microscopy (TEM). Thin foils for TEM observations were prepared from thin sections cut parallel to the compression direction. After mechanically polishing to a thickness of ∼30 μm, the specimens were thinned by ion milling at an accelerating voltage of 2–3 kV and an angle of 7°. The foils were coated with carbon to prevent charging during observations. Images were taken using weak beam, darkfield (WBDF) conditions.

2.6. Data Analysis

[14] The strain rate, $\dot{\varepsilon}$, was analyzed as a function of differential stress, σ, water fugacity, f_{H_2O}, pressure, P, and temperature, T, using a flow law of the form

$$\dot{\varepsilon} = A f_{H_2O}^r \frac{\sigma^n}{d^p} \exp\left(-\frac{E + PV}{RT}\right) \tag{2a}$$

where A is a material-dependent parameter, r is the water fugacity exponent, which is equal to zero under anhydrous conditions, n is the stress exponent, d is the grain size, p is the grain size exponent, which is zero for dislocation creep and 2 or 3 for diffusion creep, E is the activation energy, V is the activation volume, and R is the gas constant. The summation of E and PV is the activation enthalpy, Q. The effects of temperature and confining pressure on strain rate enter through the activation energy and activation volume as well as through the $f_{H_2O}^r$ term, as f_{H_2O} is a function of temperature and confining pressure. For dislocation creep, strain rate is independent of grain size, so that the flow law can be simplified to

$$\dot{\varepsilon} = A f_{H_2O}^r \sigma^n \exp\left(-\frac{Q}{RT}\right) \tag{2b}$$

In this study on coarse-grained clinopyroxenite, all deformation experiments were carried out in the dislocation creep regime such that equation (2b) was used for analysis of all the deformation data.

3. Experimental Results

[15] The experimental conditions for nine deformation runs are listed in Table 1. For each creep test in a deformation experiment, the sample was deformed by at least 1% strain to ensure that creep rate reached a steady value. As demonstrated by *Zimmerman and Kohlstedt* [2004, Figure 7], a steady state can be reached in <1% strain in a constant stress (creep) experiment even though >10% strain may be required in a constant strain rate test. This point is amplified in Appendix A.

[16] To determine the time required to fully saturate a sample with water, we carried out a creep test in which a differential stress was applied as soon as the desired T, P condition was reached; a constant creep rate was reached in less than 2.5 hours. Therefore, for deformation experiments

conducted under hydrous conditions, all of the samples were first annealed at temperature and pressure for 5 hours prior to the creep test. For all of the samples deformed under hydrous conditions, water vapor was detected in the capsule at the end of the experiment indicating that the water activity is close to unity. A thin layer of bright green NiO was found between the talc and the Ni capsule, indicating that the oxygen fugacity was buffered close to the Ni/NiO oxygen buffer ($\sim 10^{-2.7}$ Pa at the investigated confining pressures).

3.1. Water Fugacity Exponent

[17] Creep results for the nine samples are summarized in Table 2. Results from samples deformed at different confining pressures but the same temperature were used to calculate the water fugacity exponent and stress exponent. In Figure 2, data from six experiments are plotted to illustrate the effect of water fugacity on strain rate. All six experiments were conducted at a temperature of 1473 K and a water fugacity of either 140 or 280 MPa (i.e., a confining pressure of either 150 or 300 MPa; [see *Mackwell and Kohlstedt*, 1990]). A nonlinear least squares fit to the creep data following equation (2a) yields a water fugacity exponent of $r = 3.0 \pm 0.6$, a stress exponent of $n = 2.7 \pm 0.3$, and an activation volume of $V = 0$ m^3/mol. In Figure 2, the creep rate increases with increasing confining pressure due to the associated increase in water fugacity. At a given temperature and differential stress under hydrous conditions, samples deformed at a confining pressure of 300 MPa creep $\sim$4 times faster than samples deformed at 150 MPa.

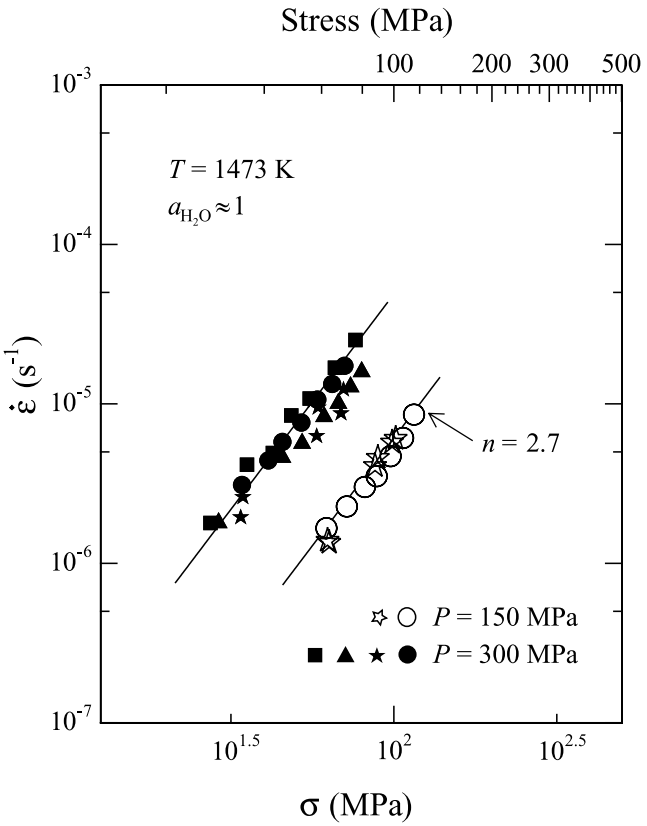

Figure 2. Log-log plot of strain rate versus stress for samples deformed at two confining pressures, 150 and 300 MPa, under hydrous conditions at 1473 K. Data are from samples PI-1196 (solid circles), PI-1197 (solid squares), PI-1209 (solid triangles), PI-1211 (open circles), PI-1215 (open stars), and PI-1216 (solid stars). The straight lines are nonlinear least squares fits to the data.

3.2. Activation Enthalpy

[18] Results from samples deformed at different temperatures were used to evaluate the activation energy for dislocation creep under hydrous conditions. In Figure 3, data from three experiments are plotted to illustrate the effect of temperature on strain rate. All three experiments were conducted at a confining pressure of 150 MPa and either 1448 or 1473 K. A nonlinear least squares fit yields an activation energy of $Q = 705 \pm 40$ kJ/mol using a stress exponent of $n = 2.7$.

[19] Data from an experiment conducted at a confining pressure of 300 MPa and temperatures from 1373 to 1448 K are plotted in Figure 4. A nonlinear least squares fit yields an activation energy of $Q = 630 \pm 40$ kJ/mol with the stress exponent fixed at $n = 2.7$.

[20] To have a better look at the activation energy for dislocation creep at both confining pressures, an Arrhenius plot is presented in Figure 5. For experiments conducted at a confining pressure of 150 MPa, strain rates obtained at differential stresses from 114 to 115 MPa were normalized to a differential stress of 100 MPa using a stress exponent $n = 2.7$. For the sample deformed at a confining pressure of 300 MPa, strain rates obtained at differential stresses from 115 to 205 MPa were normalized to a differential stress of 200 MPa using $n = 2.7$. The Arrhenius plot yields the same values for activation energy as the nonlinear least squares fits in Figures 3 and 4.

3.3. Water Content of Starting Material and Deformed Samples

[21] FTIR spectra were obtained from selected crack-free regions of grains within the clinopyroxenite for the starting material and most of the deformed samples. Because the orientations of crystals in clinopyroxene aggregates are random and absorption spectra depend on crystallographic orientation, the highest water content calculated from the spectra for each sample is taken to be the actual water content in that sample. In Figure 6, infrared spectra from three deformed clinopyroxene aggregates as well as an undeformed clinopyroxene aggregate are shown on a plot of absorption coefficient versus wave number. Samples deformed under hydrous conditions have hydroxyl concentrations ranging from 218 to 750 H/10^6 Si (9 to 31 ppm wt H_2O) on the basis of the *Paterson* [1982] calibration and 78 to 220 H/10^6 Si (3 to 10 ppm wt H_2O) on the basis of the *Bell et al.* [1995] calibration for confining pressures from 150 to 300 MPa. To illustrate the hydroxyl incorporation in clinopyroxene during an experiment, an infrared spectrum for the starting material is also shown in Figure 6. It is clear from a comparison of the spectra that the water content increases significantly during the hydrous anneal prior to the start of a deformation experiment.

[22] In all spectra from deformed samples, two characteristic bands are present, as shown in Figure 6. One band is close to a wave number of 3644 cm^{-1}, and the other is near a wave number of 3458 cm^{-1}. The band at 3644 cm^{-1} is

Table 2. Creep Results for Clinopyroxene Aggregates

Experiment	T,[a] K	Stress, MPa	Strain Rate, s^{-1}
PI-1125	1473	196.5	7.3×10^{-7}
		229.3	1.1×10^{-6}
		244.8	1.5×10^{-6}
		260.3	2.1×10^{-6}
PI-1196	1473	34.2	3.1×10^{-6}
		41.2	4.4×10^{-6}
		45.5	5.8×10^{-6}
		52.1	7.7×10^{-6}
		58.3	1.1×10^{-5}
		64.6	1.3×10^{-5}
		70.5	1.7×10^{-5}
PI-1197	1473	35.5	4.2×10^{-6}
		42.5	4.9×10^{-6}
		48.4	8.5×10^{-6}
		55.2	1.1×10^{-5}
		66	1.7×10^{-5}
		27.3	1.8×10^{-6}
		76.2	2.5×10^{-5}
PI-1209	1473	45.5	4.8×10^{-6}
		52.3	5.9×10^{-6}
		61.1	8.6×10^{-6}
		67.6	1.0×10^{-5}
		73.6	1.3×10^{-5}
		80	1.7×10^{-5}
PI-1211	1473	62.1	1.7×10^{-6}
PI-1211	1200	71.7	2.3×10^{-6}
		81.4	3.0×10^{-6}
		88.6	3.5×10^{-6}
		97.7	4.7×10^{-6}
		106.7	6.1×10^{-6}
		115.2	8.6×10^{-6}
PI-1215	1473	89.3	4.6×10^{-6}
		101.3	6.0×10^{-6}
		63.3	1.3×10^{-6}
		87.5	4.1×10^{-6}
		62.6	1.4×10^{-6}
		98.7	5.7×10^{-6}
PI-1216	1473	58.5	9.5×10^{-6}
		34.4	2.6×10^{-6}
		70	1.2×10^{-5}
		58	6.3H 10^{-6}
		33.9	1.9×10^{-6}
		68.8	8.7×10^{-6}
PI-1219	1448	77.6	9.9×10^{-7}
		102.2	2.2×10^{-6}
		114.2	2.8×10^{-6}
PI-1224	1448	78.1	6.3H 10^{-6}
		102.7	8.9×10^{-6}
		114	1.1×10^{-5}
	1423	102.1	3.0×10^{-6}
		126	4.6×10^{-6}
		148.8	8.6×10^{-6}
	1398	148.6	3.2×10^{-6}
PI-1224	1398	171.5	4.8×10^{-6}
		193.4	7.8×10^{-6}
	1373	204.6	3.7×10^{-6}
		227	5.0×10^{-6}

[a] T is temperature.

sharper and more intense than the one at 3458 cm^{-1}, and its height increases with increasing water content.

3.4. Microstructural Observations

[23] Figure 7 shows the microstructures of the starting material and a sample deformed under hydrous conditions. The average grain size is essentially the same in undeformed and deformed samples (both are 530 ± 20 μm). Deformed samples show some undulatory extinction features, which are characteristic of deformation by dislocation creep. Grain boundaries in the deformed sample have irregular shapes, while grains are polygonal and grain boundaries are straight in the starting material. Compared with the starting material, the deformed sample has more cracks due to the pressure release and temperature decrease after deformation. In the deformed sample, silica-rich inclusions, often accompanied by pores, are found within the grains. Similar features have been reported earlier for diopside, the so-called early partial melting precipitates [e.g., *Jaoul and Raterron*, 1994]. In our samples, because of cracks in the starting material, silica-rich fluid may form in the cracks with the existence of free water followed by precipitation of excess silica along the cracks. After the closure of cracks the precipitates are trapped within the grains as planar arrays of inclusions. Features indicating dynamic recrystallization and partial melting of the samples were not detected.

[24] Over twenty TEM images were taken of both wet and dry samples after deformation. In Figure 8, one example is shown for each type of sample. These samples were deformed at the same temperature and confining pressure but different differential stresses. The dislocations are more tangled in the dry sample than in the wet one. In the wet sample, subgrain boundaries are more numerous and the dislocation density lower. The dislocation density in the wet sample is lower than that in the dry sample because the stress was smaller in the former. The high density of subgrain boundaries in the wet sample indicates that dislocation climb is more efficient under hydrous conditions.

4. Discussion

4.1. Dependence of Sample Strength on Water Fugacity

[25] From equation (2a), confining pressure affects strain rate in two ways, explicitly through the PV term and implicitly through the water fugacity term. These two effects have opposite influences on strain rate. Over the confining pressure range used in this study, the PV term is much smaller than the activation energy E. A nonlinear least squares fit to our data yields $V = 0$ m^3/mol; therefore, we will neglect the PV term.

[26] By taking the average value for activation energy reported in Figures 3 and 4, we obtain the following flow law for dislocation creep of clinopyroxene aggregates under hydrous conditions:

$$\dot{\varepsilon} = 10^{6.7\pm0.1}\sigma^{2.7\pm0.3} f_{H_2O}^{3.0\pm0.6} \exp\left(-\frac{670 \pm 40 \text{ kJ/mol}}{RT}\right) \quad (3)$$

where $\dot{\varepsilon}$ is in s^{-1}, σ and f_{H_2O} are in MPa, and T is in K. We can see from equation (3) that water fugacity has a significant effect on dislocation creep rate of clinopyroxenite. In Figure 9, $\dot{\varepsilon}$ is plotted against water fugacity on a log-log scale to illustrate effect of water fugacity on creep rate.

[27] It should be noted that, because of the limited range of water fugacity that could be explored, the activation volume obtained from the nonlinear least squares fit is not highly accurate. Although the value of V does not significantly influence the value of r (for example, if $V = 20 \times 10^{-6}$ m^3/mol, then $r = 3.1$), a robust value for V is required

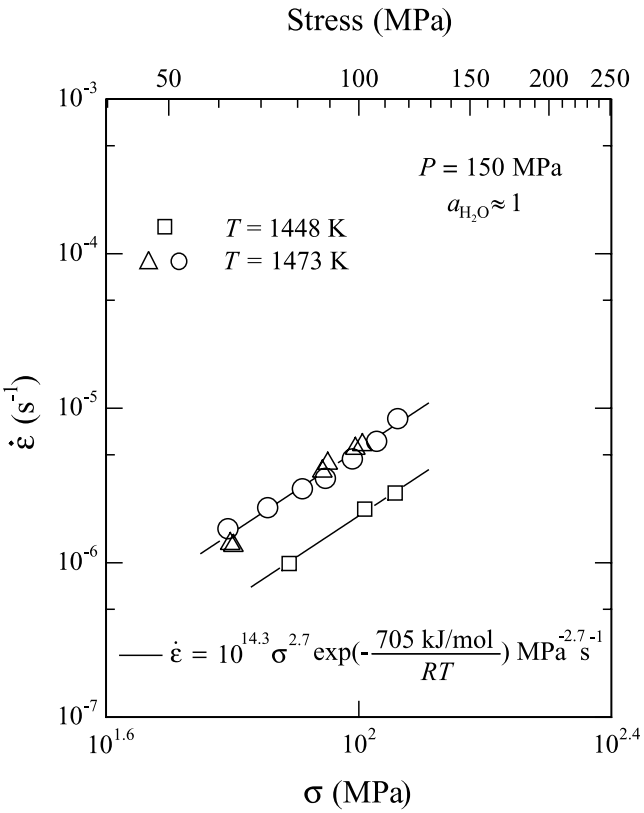

Figure 3. Log-log plot of strain rate versus stress for samples deformed under hydrous conditions at a confining pressure of 150 MPa for two different temperatures, 1448 and 1473 K. The fit yields Q = 705 ± 40 kJ/mol, with stress exponent n fixed to be 2.7. Data are from samples PI-1211 (open circles), PI-1215 (open triangles), and PI-1219 (open squares).

to extrapolate laboratory results to high pressures. For the P-T conditions at the base of the continental crust, an activation volume of 0 m^3/mol yields a strain rate a factor of ~10 larger than that obtained using a value of 20×10^{-6} m^3/mol.

4.2. Water-Weakening Mechanism

[28] In Figure 10, the plot of strain rate versus differential stress compares the creep behavior of wet and dry Sleaford Bay clinopyroxenite. The flow law for dry clinopyroxenite is from *Bystricky and Mackwell* [2001], and the flow laws for wet aggregates are from *Boland and Tullis* [1986] and this study. The samples used in all three studies are from Sleaford Bay. The samples in the *Boland and Tullis* [1986] study are somewhat stronger than ours, possibly because, in their experiments, insufficient time was allowed for H to diffuse into and saturate the samples before deformation was initiated. Wet clinopyroxene flows more than 100 times faster than dry clinopyroxene at a water fugacity of ~300 MPa for the stress and temperature ranges investigated in this study. Clearly, the effect of water on dislocation creep of clinopyroxenite is significant.

[29] What is the mechanism involved in this large water-weakening effect? *Griggs* [1974] pointed out that in quartz the presence of water hydrolyzes Si-O bonds by the reaction Si-O-Si + H_2O ⇒ Si-OH OH-Si; he argued that this action will make the glide of dislocations easier thus weakening the material. Alternatively, water can influence creep rate through its effect on climb. At relatively low-temperature high-stress conditions, dislocation glide contributes more to the creep process than does dislocation climb, but at higher temperature (in general, higher than ~2/3T_m, where the melting point T_m is ~1573 K for wet clinopyroxene), climb becomes more important than glide [e.g., *Weertman*, 1999]. Since dislocation climb involves diffusion of ions, the rate of climb will be enhanced by higher concentrations of point defects and thus higher diffusivities of ionic species with the presence of water. In our study, we emphasize the latter water-weakening mechanism on the basis of the following arguments:

[30] 1. *Mei and Kohlstedt* [2000a] argued that, in olivine aggregates, the concentration of point defects on the silicon sublattice, and thus the diffusivity of silicon (the rate-controlling ionic species in diffusion creep of olivine), are significantly enhanced with the presence of water. Hence the rate of diffusion creep of olivine increases systematically with the increase of water fugacity. *Mei and Kohlstedt* [2000b] also explained the water-weakening effect on dislocation creep of olivine from the climb-controlled creep point of view.

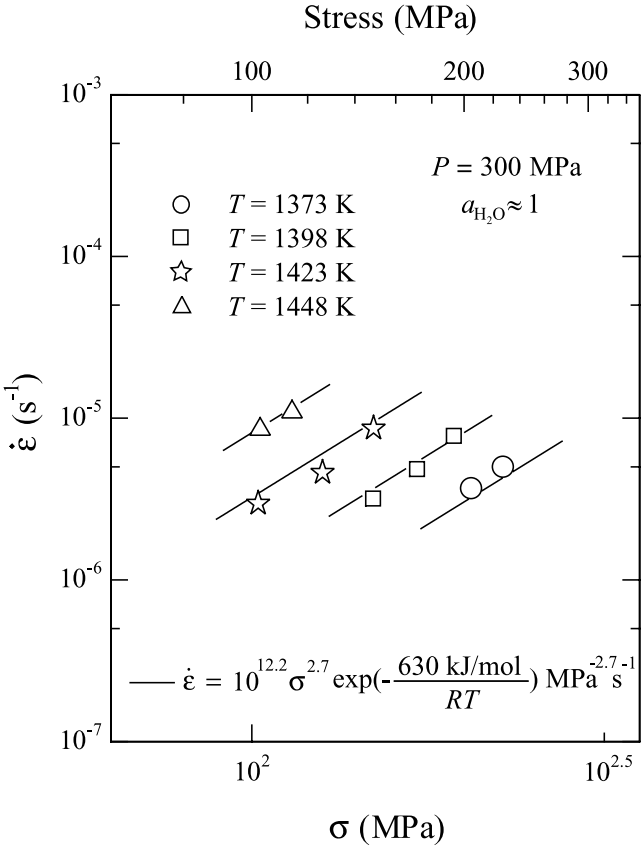

Figure 4. Log-log plot of strain rate versus stress for sample PI-1224 deformed under hydrous conditions at a confining pressure of 300 MPa and four different temperatures, 1373, 1398, 1423 and 1448 K. The fit yields Q = 630 ± 40 kJ/mol with the stress exponent n fixed to be 2.7.

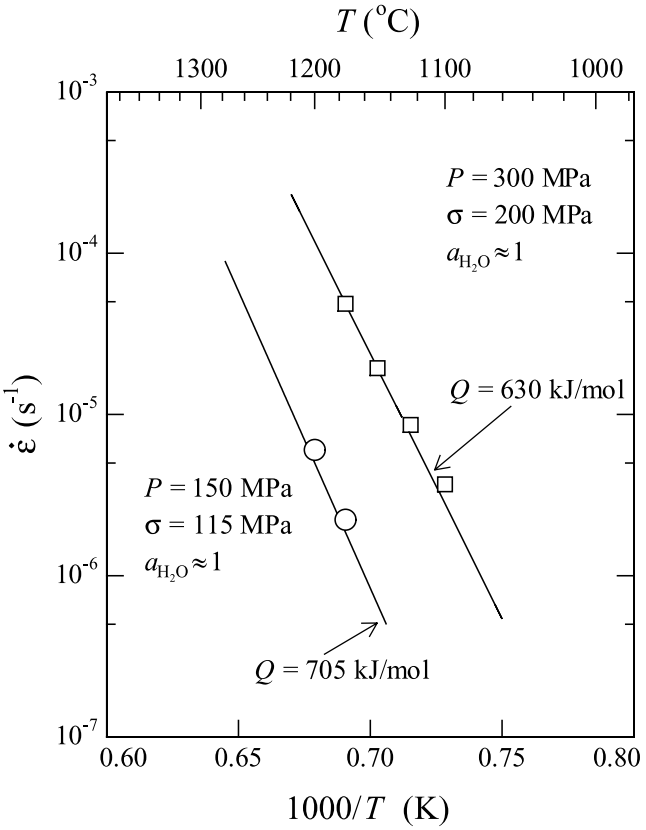

Figure 5. Arrhenius plot of log strain rate versus inverse temperature for samples deformed at confining pressures of 150 and 300 MPa. Data are from samples PI-1211 (1473 K) and PI-1219 (1448 K) (open circles) and PI-1224 (open squares). The lines are obtained from the flow laws generated using the entire data set.

[31] 2. *Hier-Majumder et al.* [2005] observed a pronounced water weakening of clinopyroxene aggregates in the diffusion creep regime. They argued that, in the presence of water the majority point defects in clinopyroxene are water, derived and, consequently, the concentrations of these point defects as well as those responsible for diffusion on the cation and anions sublattices are functions of water fugacity. As a result, the strength of clinopyroxene decreases with increasing water fugacity.

[32] 3. In this study, from the TEM images taken of clinopyroxene aggregates deformed under dry and wet conditions (Figure 8), the dislocations are frequently tangled and fewer subgrain boundaries appear in samples deformed under dry conditions. In contrast, in samples deformed under hydrous conditions, subgrain boundaries are numerous. These observations indicate that under wet conditions, dislocation climb is much more efficient than it is under dry conditions in clinopyroxene.

[33] 4. As pointed out by *Poirier* [1985], "the 'natural' stress dependence for any climb-controlled recovery creep is a power law with stress exponent $n = 3$." Thus the value for the stress exponent determined in this study for creep of clinopyroxene under water-saturated conditions, $n = 2.7 \pm 0.3$, is consistent with a climb-controlled dislocation creep mechanism.

[34] It is from this perspective that we emphasize the importance of water on enhancing the rate of diffusion of the slowest species and thus the rate of creep controlled by dislocation climb.

4.2.1. Dislocation Climb Mechanism

[35] The climb of a dislocation involves the formation and migration of jogs along the dislocation line. The movement of jogs is associated with emitting or absorbing vacancies. These jogs can be neutral, positively charged, or negatively charged, an idea originally proposed for Si and Ge [*Hirsch*, 1979, 1981] and then extended to silicates like quartz, forsterite and albite [*Hobbs*, 1984]. The formation of charged jogs is associated with dangling bonds, which are under-bonded covalent bonds at the ends of edge dislocation half planes. These dangling bonds give rise to electronic states, and, with the presence of donor or acceptor impurities, some of the empty states are filled by electrons and full states are filled by electron holes, thus forming charged dislocation lines, in other words, charged jogs [*Hirsch*, 1979, 1981; *Labusch and Schroter*, 1980]. The ionization of jogs can be written, following the Kröger-Vink notation [*Kröger and Vink*, 1956], as [*Hobbs*, 1984]

$$J^x \Leftrightarrow J^\bullet + e' \qquad J^x \Leftrightarrow J' + h^\bullet \tag{4}$$

where J^x, J', and $J^\bullet$ are neutral, negative and positive jogs, respectively, e' is an electron, and $h^\bullet$ is an electron hole, which is the defect $Fe^\bullet_{Me}$ in Fe^{3+} bearing clinopyroxenes. Since the concentration of neutral jogs is only thermally dependent and thus constant at a given temperature, the concentration of charged jogs depends only on the concentrations of electrons and holes at a certain temperature, as illustrated in the following by applying the law of mass action to equation (4):

$$[J^\bullet] \propto [h^\bullet] \qquad [J'] \propto [e'] \tag{5}$$

where the square bracket means concentration. In our study, with the presence of water, hydrogen is incorporated into clinopyroxene as hydroxyl (OH), and this incorporation process introduces new point defect species and changes the concentration of intrinsic point defects as well. As a result, the water fugacity will affect the concentration of charged jogs and thus influence the velocity of dislocation climb.

[36] The velocity of dislocation climb at a given stress depends not only on jog concentration, C_j, but also on jog mobility, μ_j. The velocity of dislocation climb, v, is given by *Hobbs* [1981]

$$\begin{aligned} v = {} & \text{constant} \times (\text{concentration of the jogs}) \\ & \times (\text{mobility of jogs}) \propto C_j \mu_j \end{aligned} \tag{6}$$

The mobility of jogs is proportional to the diffusivity of the rate-controlling ionic species [*Hirth and Lothe*, 1982], where the diffusivity of the rate-limiting ionic species can be written as the product of the diffusivity and concentration of point defects of that species. Since the presence of an impurity has an effect on the defect chemistry of a material, it can influence the mobility of jogs and thus affect the dislocation climb velocity. From *Orowan*'s [1940] equation

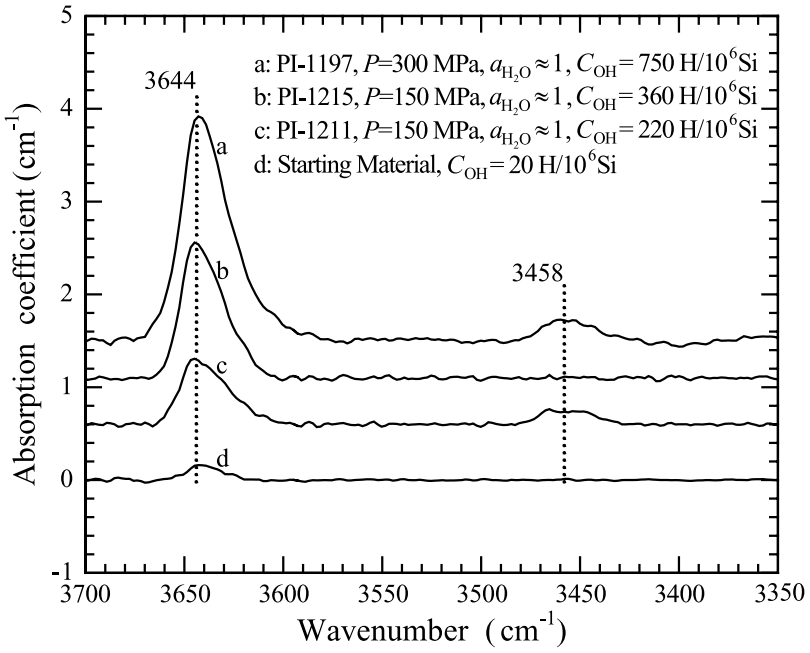

Figure 6. Fourier transform infrared spectra from samples PI-1197 (300 MPa hydrous), PI-1211 (150 MPa hydrous), and PI-1215 (150 MPa hydrous) as well as the starting material. Spectra were obtained with an unpolarized beam from selected grains within the polycrystalline clinopyroxenite. Values reported for C_{OH} are based on the Paterson calibration [*Paterson*, 1982]; the calibration of *Bell et al.* [1995] yields values of C_{OH} that are smaller by a factor of ~3.

the creep rate contributed by dislocation climb with the movement of jogs is

$$\dot{\varepsilon} \propto \rho b C_j C_p D_p \tag{7}$$

where ρ is the dislocation density, b is the Burgers vector, and C_p and D_p are the concentration and diffusivity of point defects of the rate-controlling species, respectively. The C_j term here includes all possible jog types, but, in the discussion below, we will only consider the dominant type of jogs, either positively charged, negatively charged, or neutral jogs.

4.2.2. Water-Weakening Mechanism in Dislocation Creep of Clinopyroxene

[37] In clinopyroxene, hydrogen is structurally bound as hydroxyl ions. *Skogby and Rossman* [1989], *Skogby et al.* [1990], and *Skogby* [1994] carried out a series of studies on OH incorporation in both natural and synthesized pyroxenes. They found a positive relationship between the $(Al^{3+} + Fe^{3+} + Cr^{3+})/Fe^{2+}$ ratio and OH concentration in pyroxenes. Since the hydrogen tends to bond to the under-bonded O2 position, they suggested that, with the presence of trivalent ions, OH incorporation is enhanced because the substitution of trivalent ions into the Si tetrahedral sites in pyroxenes makes the O2 sites even more under bonded. This substitution reaction involving point defects can be expressed as

$$\frac{1}{2}H_2O + \frac{1}{4}O_2 + 2FeO + Si_{Si}^{x} + O_O^{x} \Leftrightarrow Fe'_{Si} + (OH)_O^{\bullet} + FeSiO_3 \tag{8}$$

where the excess charge created by hydrogen incorporation is balanced by the charge-deficient substitution of Fe^{3+} into the Si site.

[38] In infrared studies of pyroxenes from a variety of origins, absorption bands in the 3630 to 3650 cm^{-1} region and the 3350–3520 cm^{-1} region are common [*Skogby and Rossman*, 1989; *Skogby et al.*, 1990; *Skogby*, 1994; *Bromiley et al.*, 2004]. The former appear to correlate with Fe^{3+} and Al^{3+}, while the latter correlate with Fe^{2+} [*Skogby and Rossman*,1989; *Skogby et al.*, 1990; *Skogby*, 1994]. The two absorption bands found in our wet sample also fall into these two regions (Figure 6), and the band at 3644 cm^{-1} is sharper and more intense than the band at 3458 cm^{-1}. As the concentration of OH increases, the amplitude of the band at 3644 cm^{-1} increases. Since our sample is poor in Al^{3+}, Fe^{3+} will play an important role in substituting for Si in the tetrahedral sites. Thus the two types of point defects created in equation (8) are very likely to be the majority defect species and thus control charge neutrality in clinopyroxene:

$$\left[Fe'_{Si}\right] = \left[(OH)_O^{\bullet}\right] \tag{9}$$

Hier-Majumder et al. [2005] proposed the same charge neutrality for his fine-grained clinopyroxene aggregates deformed under hydrous conditions.

[39] By combining equation (8) with equation (9) and applying the law of mass action, the concentrations of the majority point defects are

$$\left[Fe'_{Si}\right] = \left[(OH)_O^{\bullet}\right] = k a_{FeO} a_{FeSiO_3}^{-1/2} f_{O_2}^{1/8} f_{H_2O}^{1/4} \tag{10}$$

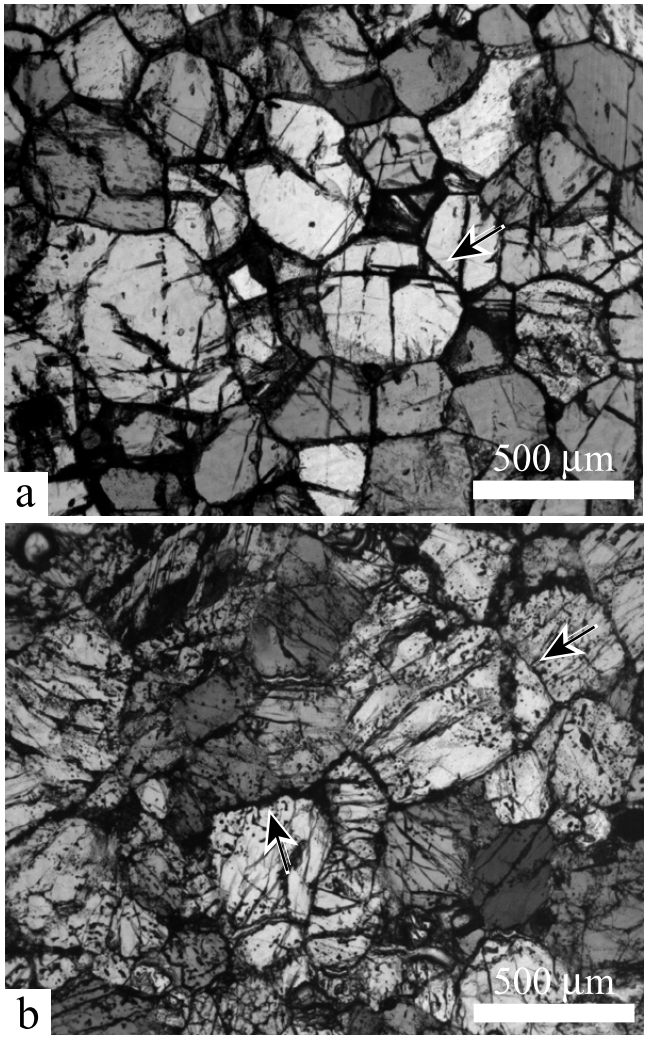

Figure 7. Polarized transmitted light micrographs of (a) the starting clinopyroxenite material and (b) a sample deformed under hydrous conditions (PI-1209) at a temperature of 1473 K and a confining pressure of 300 MPa. Grain boundaries in the deformed sample have irregular shapes, while grains are polygonal and grain boundaries are straight in the starting material (marked by arrows).

where k, the reaction constant for equation (9), is a function of temperature and pressure, a_{FeO} is the activity of FeO, a_{FeSiO_3} is the activity of $FeSiO_3$, f_{O_2} is the oxygen fugacity and f_{H_2O} is the water fugacity.

[40] Among all the possible kinds of ionic species in clinopyroxene, Si ions diffuse more slowly than Ca and O ions (for O: *Farver* [1989], *Connolly and Muehlenbachs* [1988], *Ryerson and McKeegan* [1994]; for Ca: *Dimanov et al.* [1995]; for Si: *Béjina and Jaoul* [1996]). The formation of vacancies and interstitials on the Si sublattices are given in the reactions below:

$$Si_{Si}^{x} + 2O_{O}^{x} \Leftrightarrow V_{Si}'''' + 2V_{O}^{\bullet\bullet} + SiO_2 \quad (11)$$

$$Si_{Si}^{x} \Leftrightarrow V_{Si}'''' + Si_{i}^{\bullet\bullet\bullet\bullet} \quad (12)$$

[41] In addition, with the presence of water, point defect associates can be formed by combining $(OH)_O^{\bullet}$ and vacancies [*Kohlstedt et al.*, 1996]. Two possible point defect associates are formed as follows:

$$V_{Si}'''' + 3(OH)_O^{\bullet} \Leftrightarrow \left\{ \left(3(OH)_O^{\bullet} - V_{Si}'''' \right)' \right\} \equiv (3H)_{Si}' \quad (13)$$

$$V_{Si}'''' + 4(OH)_O^{\bullet} \Leftrightarrow \left\{ \left(4(OH)_O^{\bullet} - V_{Si}'''' \right)^{x} \right\} \equiv (4H)_{Si}^{x} \quad (14)$$

where the point defects $(3H)_{Si}'$ and $(4H)_{Si}^{x}$ are referred to as hydrogarnet defects and may be important in quartz [*McLaren et al.*, 1983] and olivine also [*Beran and Putnis*, 1983]. These defects would speed up dislocation motion by introducing more silicon vacancies and reducing the activation barrier for defect motion, thus enhancing the defect mobility and dislocation climb velocity [*Hobbs*, 1984].

[42] The concentrations of the point defects in equations (11)–(14) are all functions of water fugacity. This water fugacity dependence of the concentration of each point defect can be determined following the method used in equation (10), and for the point defect species appearing in equations (8) and (11) to (14), the charge neutrality condition in equation (9) is used. The results are shown in Table 3. In Table 4, the water fugacity exponent r, which defines the dependence of the creep rate of clinopyroxene on water fugacity, is listed for different combinations of diffusion mechanism and jog type calculated from equation (7) and Table 3.

[43] From the results in Table 4 the value of $r = 9/4$ is closest to our experimentally determined water fugacity exponent of $r = 3.0 \pm 0.6$, suggesting the possibility that water weakening of clinopyroxene in the dislocation creep regime is controlled by diffusion-accommodated dislocation climb with silicon as the rate-controlling ionic species diffusing by an vacancy mechanism associated with hydrogarnet-type point defect associates. The difference between the experimental and predicted values of r may be due to two reasons: (1) Since it was only possible to investigate a relatively narrow range of water fugacity, the uncertainty in the measured value for the water fugacity exponent is relatively large, and (2) the dislocation creep process for wet clinopyroxene is oversimplified by the climb model proposed here. Multiple mechanisms may be involved in the water-weakening effect, including cross-slip of screw dislocations. However, the dislocation climb model discussed above is a first step toward understanding the water-weakening mechanism in clinopyroxene, and it is possibly an important mechanism involved in the reduction of creep strength of clinopyroxene in going from anhydrous to hydrous conditions.

4.3. Comparison to Other Minerals

[44] The influence of water on creep rate has also been studied for minerals other than clinopyroxene. In Figure 11, published dry and wet dislocation flow laws for aggregates of clinopyroxene (dry, coarse-grained natural samples: *Bystricky and Mackwell* [2001]), olivine (dry and wet, coarse-grained natural samples: *Chopra and Paterson*

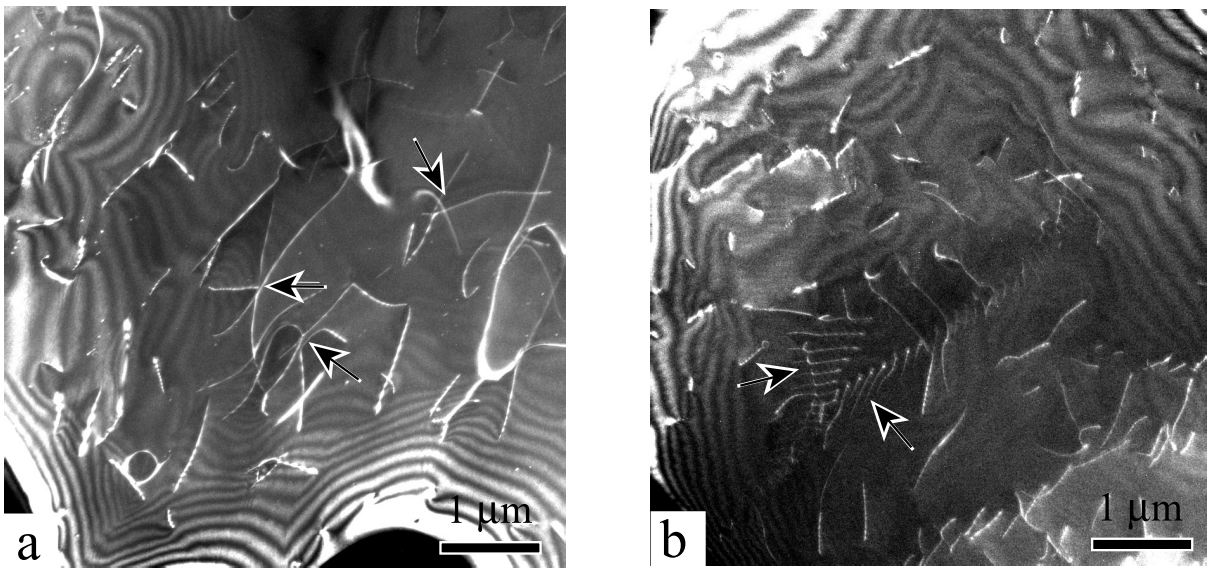

Figure 8. Weak beam, darkfield transmission electron microscopy images of dislocations in deformed samples. (a) This image of a dry sample (PI-1125) was taken along the $[11\bar{4}]$ axis with $\mathbf{g} = (\bar{2}20)$. The dislocations are often tangled (marked by arrows). (b) This image of the wet sample (PI-1209) was taken along the $[\bar{3}\ \bar{2}5]$ axis with $\mathbf{g} = (111)$. Dislocations form subgrain boundaries (indicated with arrows) more frequently than those in dry sample.

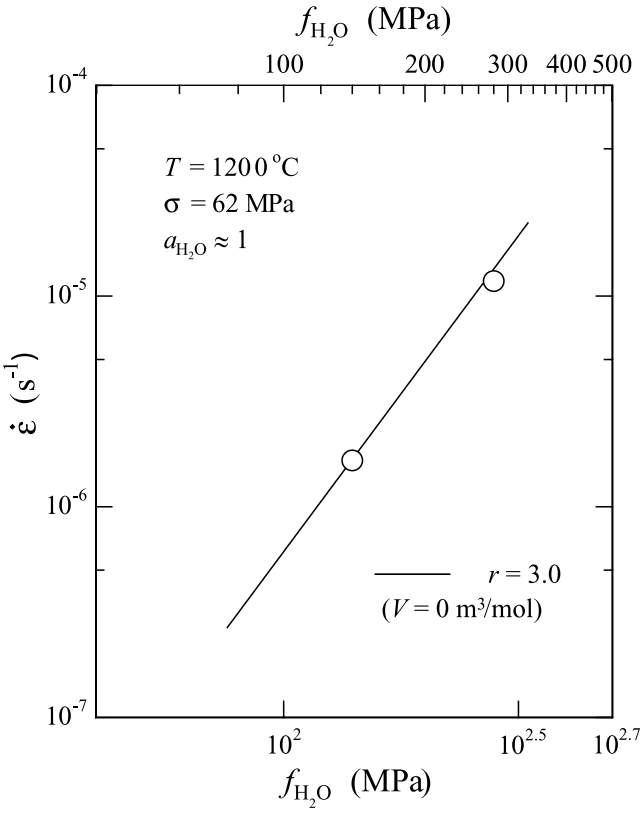

Figure 9. Log-log plot of strain rate versus water fugacity. Data points are from Figure 2 with $V = 0$ m^3/mol and stress normalized to 62 MPa. The solid line is obtained from the flow laws generated using the entire data set.

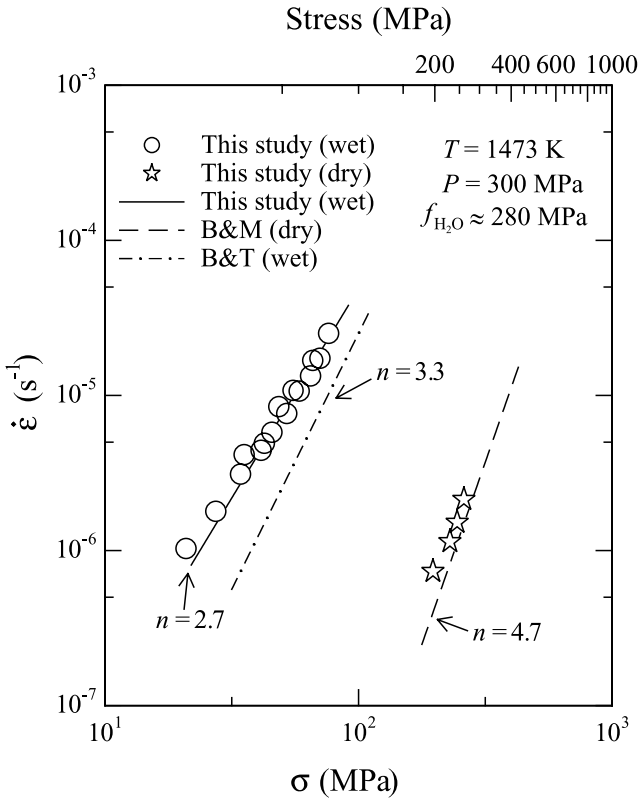

Figure 10. Comparison of our wet flow law with published dry and wet flow laws. The dry flow law is from *Bystricky and Mackwell* [2001]. The wet flow laws are from *Boland and Tullis* [1986] and this study. The data are from samples PI-1125 (open stars) as well as PI-1196 and PI-1197 (open circles).

Table 3. Water Fugacity Exponent, q, Defined in Equation (Point Defect Species) $\propto f_{H_2O}^q$; Describing the Dependence of the Concentration of Point Defect Species on Water Fugacity for the Charge Neutrality Condition $[Fe'_{Si}] = [(OH)^{\bullet}_{O}]$ in Clinopyroxene Under Hydrous Conditions[a]

	Charge Neutrality Condition $[Fe'_{Si}] = [(OH)^{\bullet}_{O}]$							
Point Defect Concentration	$[J^{\bullet}]$	$[J']$	$[Fe'_{Si}]$	$[(OH)^{\bullet}_{O}]$	$[V''''_{Si}]$	$[Si_i^{\bullet\bullet\bullet\bullet}]$	$[(3H)'_{Si}]$	$[(4H)^{x}_{Si}]$
q	−1/4	1/4	1/4	1/4	1	−1	3/2	2

[a]J is jog and V is vacancy.

[1984]), and anorthite aggregates (dry, coarse-grained samples: *Shelton and Tullis* [1981]; and wet, fine-grained synthetic samples: *Rybacki and Dresen* [2000]) are plotted together with our wet dislocation flow law for clinopyroxenite aggregates. In olivine deformed under dry conditions, fine-grained samples creep about 1 order of magnitude faster than coarse-grained natural samples in the dislocation creep regime [*Chopra and Paterson*, 1984; *Mei and Kohlstedt*, 2000b; *Hirth and Kohlstedt*, 1995; *Hirth and Kohlstedt*, 2003]. However, under wet conditions the strengths of fine-grained and coarse-grained samples are essentially identical [*Chopra and Paterson*, 1984; *Mei and Kohlstedt*, 2000b]. Under dry conditions the von Mises criterion is fulfilled with the help of grain boundary sliding, which is a grain-size dependent process [*Paterson*, 1969]. With the presence of water, dislocation climb becomes more important and takes the role of satisfying the von Mises criterion [*Hirth and Kohlstedt*, 2003]. Thus the strain rate of finer grained olivine aggregates in the dislocation creep regime is grain-size dependent under dry conditions but not under hydrous conditions. In our comparison of the creep behavior of clinopyroxene aggregates with the flow behavior of other minerals, we assume that this situation applies not only to olivine but also to clinopyroxene and anorthite aggregates; a clear grain size dependence is observed in the work of *Bystricky and Mackwell* [2001] on clinopyroxenite, as their fine-grained samples creep about 10 times faster than their coarse-grained samples. Thus we suggest that the strength of fine-grained anorthite will be comparable to that of coarse-grained anorthite under hydrous conditions.

[45] One can see from Figure 11 that the water-weakening effect is more significant in clinopyroxene than it is in olivine and anorthite. Dry clinopyroxene is slightly stronger than dry olivine, but wet clinopyroxene is much weaker than wet olivine. As two of the major minerals in Earth's lower crust, anorthite is much weaker than clinopyroxene when they are both dry; but in a water-saturated atmosphere at a confining pressure of 300 MPa, the strengths of clinopyroxene and anorthite are comparable. Thus the flow of clinopyroxene may contribute significantly to the deformation of the lower crust when the water fugacity is high.

[46] As a conclusion, the rate of dislocation creep of coarse-grained clinopyroxene aggregates is highly enhanced in the presence of water. At a temperature of 1473 K, a confining pressure of 300 MPa and a given differential stress, wet clinopyroxene flows over 100 times faster than dry clinopyroxene. The creep rate of clinopyroxene under hydrous conditions depends on the water fugacity to the 3.0 ± 0.6 power, with an activation volume of 0 m^3/mol, within the investigated range of confining pressure of 150 to 300 MPa. We suggest that one of the possible water-weakening mechanism is dislocation climb associated with negative jogs and the diffusion of silicon ions (rate-controlling ionic species) with charge neutrality given by $[Fe'_{Si}] = [(OH)^{\bullet}_{O}]$. Among the three major minerals in Earth's lower crust, the water-weakening effect is much more significant for clinopyroxene than for olivine and anorthite.

5. Geological Implications

[47] Our experimental study explored the dependence of strain rate of coarse-grained clinopyroxenite on water fugacity in the dislocation creep regime. Extrapolation of our laboratory data to the geological conditions in Earth's lower crust is critical for constraining the strength of Earth's deep crust at localities where water-rich conditions exist. However, the mechanical behavior of a lower-crustal lithology is more complex than in our experiments, as clinopyroxene is rarely present as a monominerallic aggregate. Thus its contribution to the strength of a multiple-phase assemblage must be considered. Evidence from lower-crustal xenoliths derived from many continents demonstrate that the mineral assemblages are dominated by pyroxenes and plagioclase [*Montanini and Tribuzio*, 2001; *Kempton et al.*, 2001; *Upton et al.*, 2001]. Thus the mechanical behavior of the combination of plagioclase and pyroxene is expected to govern the creep strength of Earth's lower crust. Rules describing the flow strength for multiple-phase rocks such as those proposed by *Tullis et al.* [1991] emphasize the effects of volume fraction, creep strength, and phase distribution on overall flow strength. Their predicted flow stresses fit reasonably well with the experimentally determined strength for diabase (~64 vol% pyroxene, ~36 vol%

Table 4. Water Fugacity Exponent, r, for the Creep Rate of Clinopyroxene Aggregates Under Hydrous Conditions According to Different Diffusion Mechanisms and Jog Types[a]

Rate-Controlling Ionic Species	Concentration of Associated Point Defects	Dependence of Creep Rate on $f_{H,O}$, r		
		Positively Charged $J^{\bullet}$	Negatively Charged J'	Neutral J^x
Si	$[V''''_{Si}]$	3/4	5/4	1
	$[Si_i^{\bullet\bullet\bullet\bullet}]$	−5/4	−3/4	−1
	$[(3H)'_{Si}]$	5/4	7/4	3/2
	$[(4H)^{x}_{Si}]$	7/4	9/4	2

[a]J is jog and V is vacancy.

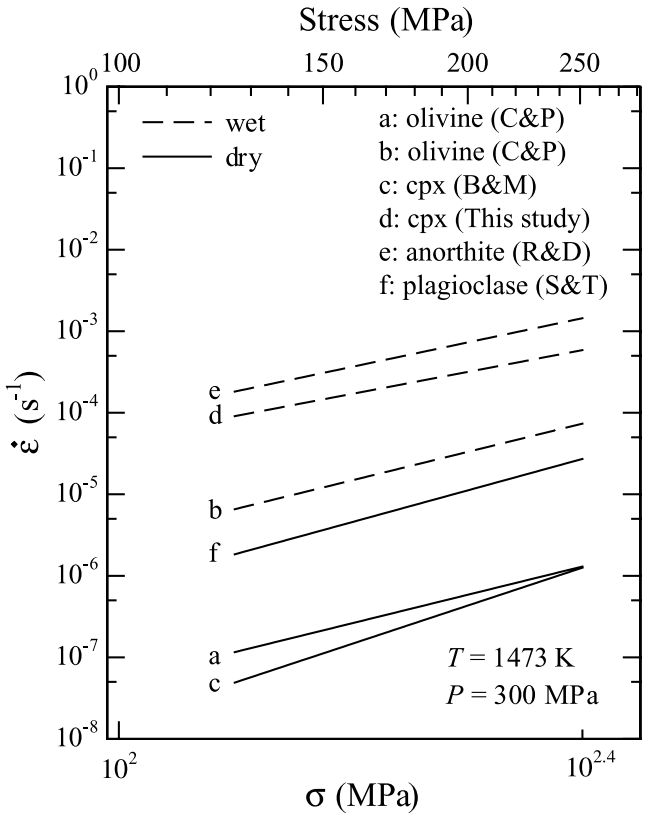

Figure 11. Comparison of the strength of olivine aggregates [*Chopra and Paterson*, 1984], clinopyroxene aggregates [*Bystricky and Mackwell*, 2001 and this study], and anorthite aggregates [*Shelton and Tullis*, 1981; *Rybacki and Dresen*, 2000] deformed under anhydrous and hydrous conditions in the dislocation creep regime at a temperature of 1473 K and a confining pressure of 300 MPa.

plagioclase). The model for creep of multiple-phase rocks presented by *Ji and Xia* [2002], although different in detail from that of *Tullis et al.* [1991], yields similar results. In Figure 12, we compare experimentally determined flow laws for Maryland diabase (~56 vol % plagioclase, ~43 vol% clinopyroxene) and Columbia diabase (~70 vol% plagioclase, ~23 vol% clinopyroxene) [*Mackwell et al.*, 1998], predicted flow laws for rocks of these plagioclase to clinopyroxene ratios calculated from the mixture rules of *Tullis et al.* [1991], and the experimentally determined flow laws for dry clinopyroxene [*Bystricky and Mackwell*, 2001] and dry plagioclase [*Shelton and Tullis*, 1981]. Columbia diabase is weaker than Maryland diabase, consistent with the flow model, taking into account its higher plagioclase content. The experimentally determined flow strengths of diabase rocks fit very well with the theoretical models and, furthermore, both experimental and theoretical flow laws fall between the creep strengths of the rock-forming end-members, which is well predicted by the two-phase flow model.

[48] However, in 'wet' regions in Earth's lower crust, it is another story. Figure 11 clearly shows that the strength of clinopyroxene decreases by over 2 magnitudes with the presence of water at 300 MPa confining pressure and is comparable to the strength of wet anorthite aggregates at the same water fugacity. Since rocks of diabase compositions cannot be deformed in the laboratory under hydrous conditions without the formation of a substantial amount of melt, experiments on single-phase samples are crucial for evaluating the creep behavior of polyphase rocks. Water does not distribute/partition evenly among different phases. Studies on the concentration levels of hydroxyl in nominally anhydrous upper mantle minerals demonstrate that the hydrogen contents of natural samples vary in the following order: diopside > enstatite > olivine > garnet [*Ingrin and Skogby*, 2000]; that is, diopside incorporates more hydrogen than the other phases under wet conditions. However, very little information exists on water partitioning between plagioclase and clinopyroxene. On the basis of recent research on the water concentration in feldspars of various compositions from different geological settings, the structural OH contained in feldspars is 510 ppm H_2O [*Johnson and Rossman*, 2003, 2004]. This value is about 4 times smaller than that in mantle derived and synthesized clinopyroxene samples [*Skogby et al.*, 1990; *Smyth et al.*, 1991; *Bell and Rossman*, 1992; *Skogby*, 1994; *Katayama and Nakashima*, 2003]. There is a lack of direct comparison of hydrogen concentration in clinopyroxene and plagioclase from the same locality. In Earth's deep crust (~35 km) the water fugacity can be as high as 700 MPa under water-saturated conditions; therefore clinopyroxene could be

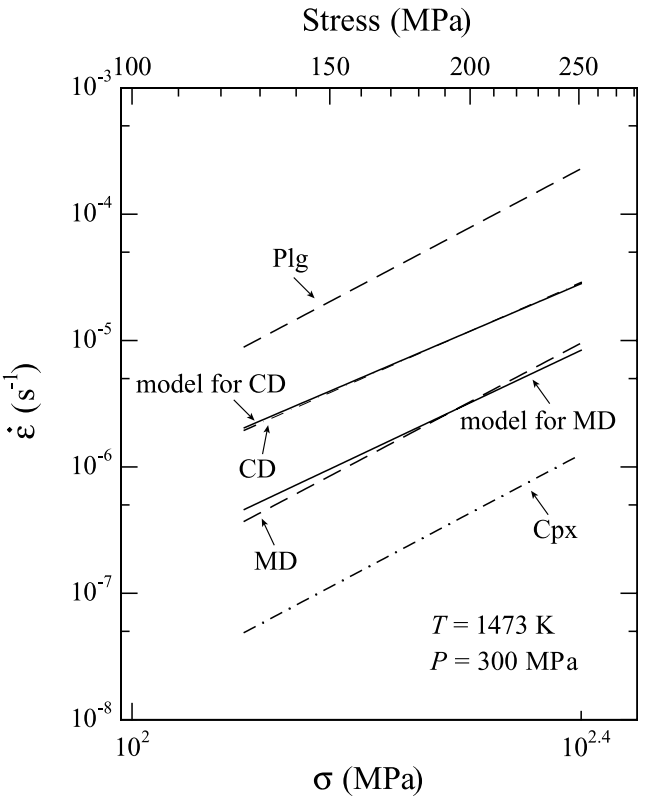

Figure 12. Comparison of experimentally determined strength of dry anorthite aggregates [*Shelton and Tullis*, 1981], dry clinopyroxene aggregates [*Bystricky and Mackwell*, 2001], and dry Columbia diabase (CD) and Maryland diabase (MD) [*Mackwell et al.*, 1998] with predicted strength of dry rocks with mineralogies similar to those of Columbia and Maryland diabase calculated on the basis of the two-phase flow model of *Tullis et al.* [1991].

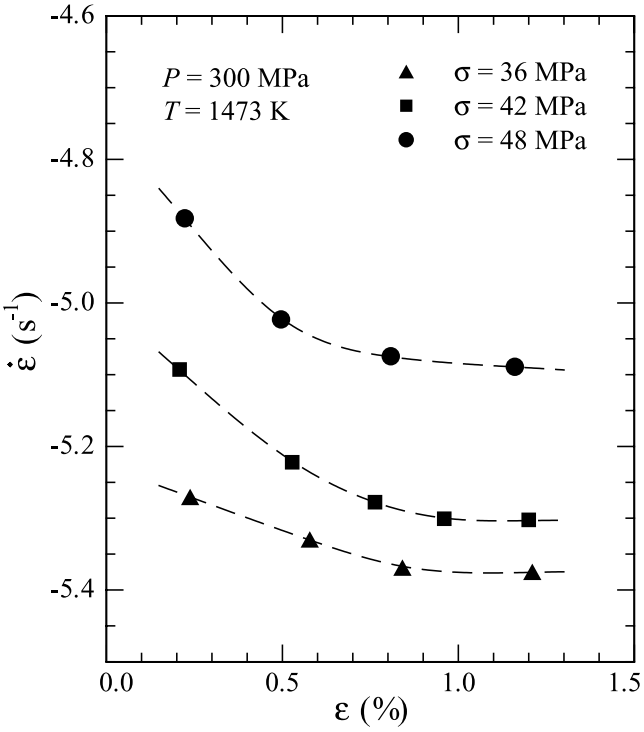

Figure A1. Semilog plot of strain rate versus strain for three creep tests in one deformation experiment, PI-1197. The dashed lines are the best fit to the data.

weaker than plagioclase in the presence of water in the deep crust and have a significant effect on the creep strength of plagioclase-pyroxene-dominated rocks. According to the strength rules of mixtures [*Tullis et al.*, 1991], the creep strength of wet diabase will fall between the creep strengths of wet clinopyroxene and wet plagioclase, which will be close to each other (see Figure 11). Consequently, the strength of wet diabase should be close to that of its end-member minerals. Therefore the mechanical behavior of wet clinopyroxene will be a critical element in modeling the creep strength of Earth's lower crust under hydrous conditions.

Appendix A

[49] To verify that our creep results represent a steady state, strain rate is plotted versus strain following three steps in stress during one creep experiment. In each case, after a change in stress a constant value of strain rate is attained at a strain of <1%, as illustrated in Figure A1.

[50] **Acknowledgments.** The authors wish to thank Terry Tullis, Steve Mackwell, and Ian Jackson for providing sample material for our experiments, Mark Zimmerman for guidance with high-pressure experiments, Saswata Hier-Majumder for sharing experimental results, Justin Hustoft for help with grain-size measurements, Sylvie Demouchy for help with FTIR analyses, and Ellery Frahm for technical assistance with electron microprobe analyses. We also wish to acknowledge the Electron Microprobe Laboratory and Charfac Facility at the University of Minnesota. Insightful reviews helped improve the manuscript. Finally, we are grateful to the NSF for research support through grant EAR- 0439747.

References

Béjina, F., and O. Jaoul (1996), Silicon self-diffusion in quartz and diopside measured by nuclear micro-analysis methods, *Phys. Earth Planet. Inter.*, *97*, 145–162.

Bell, D. R., and G. R. Rossman (1992), Water in Earth's mantle: The role of nominally anhydrous minerals, *Science*, *255*, 1391–1397.

Bell, D. R., P. D. Ihinger, and G. R. Rossman (1995), Quantative analysis of trace OH in garnet and pyroxenes, *Am. Mineral.*, *80*, 465–474.

Beran, A., and A. Putnis (1983), A model of the OH positions in olivine, derived from infrared spectroscopic investigations, *Phys. Chem. Miner.*, *9*, 57–60.

Boland, J. N., and T. E. Tullis (1986), Deformation behavior of wet and dry clinopyroxenite in the brittle to ductile transition region, in *Mineral and Rock Deformation: Laboratory Studies*, *Geophys. Monogr. Ser.*, vol. 36, edited by B. E. Hobbs and H. C. Heard, pp. 35–49, AGU, Washington, D. C.

Bromiley, G. D., H. Keppler, C. McCammon, F. A. Bromiley, and S. D. Jacobsen (2004), Hydrogen solubility and speciation in natural, gem-quality chromian diopside, *Am. Mineral.*, *89*, 941–949.

Bystricky, M., and S. Mackwell (2001), Creep of dry clinopyroxene aggregates, *J. Geophys. Res.*, *106*, 13,443–13,454.

Chopra, P. N., and M. S. Paterson (1984), The role of water in the deformation of dunite, *J. Geophys. Res.*, *89*, 7861–7876.

Connolly, C., and K. Muehlenbachs (1988), Contrasting oxygen diffusion in nepheline, diopside and other silicates and their relevance to isotopic systematics in meteorites, *Geochim. Cosmochim. Acta*, *52*, 1585–1591.

Dimanov, A., O. Jaoul, and V. Sautter (1995), Calcium self-diffusion in natural diopside single crystals, *Geochim. Cosmochim. Acta*, *60*, 4095–4106.

Dimanov, A., M. P. Lavie, G. Dresen, J. Ingrin, and O. Jaoul (2003), Creep of polycrystalline anorthite and diopside, *J. Geophys. Res.*, *108*(B1), 2061, doi:10.1029/2002JB001815.

Farver, J. R. (1989), Oxygen self-diffusion in diopside with application to cooling rate determinations, *Earth Planet. Sci. Lett.*, *92*, 386–396.

Frost, H. J., and M. F. Ashby (1982), *Deformation- Mechanism Maps: The Plasticity and Creep of Metals and Ceramics*, 167 pp., Elsevier, New York.

Gifkins, R. C. (1970), *Optical Microscopy of Metals*, Elsevier, New York.

Griggs, D. T. (1974), A model of hydrolytic weakening in quartz, *J. Geophys. Res.*, *79*, 1653–1661.

Hier-Majumder, S., S. Mei, and D. L. Kohlstedt (2005), Water weakening of clinopyroxenite in diffusion creep, *J. Geophys. Res.*, *110*, B07406, doi:10.1029/2004JB003414.

Hirsch, P. B. (1979), A mechanism for the effect of doping on dislocation mobility, *J. Phys. Colloq.*, *40*(C6), 117–121.

Hirsch, P. B. (1981), Plastic deformation and electronic mechanisms in semiconductors and insulators, *J. Phys. Colloq.*, *42*(C3), 149–159.

Hirth, G., and D. L. Kohlstedt (1995), Experimental constraints on the dynamics of the partially molten upper mantle: 2. Deformation in the dislocation creep regime, *J. Geophys. Res.*, *100*, 15,441–15,449.

Hirth, G., and D. L. Kohlstedt (2003), Rheology of the upper mantle and the mantle wedge: A view from the experimentalists, in *Inside the Subduction Factory*, *Geophys. Monogr. Ser.*, edited by J. Eiler, *138*, pp. 83–105, AGU, Washington, D. C.

Hirth, J. P., and J. Lothe (1982), *Theory of Dislocations*, pp. 555–580, John Wiley, Hoboken, N. J.

Hobbs, B. E. (1981), The influence of metamorphic environment upon the deformation of materials, *Tectonophysics*, *78*, 335–383.

Hobbs, B. E. (1984), Point defect chemistry of minerals under a hydrothermal environment, *J. Geophys. Res.*, *89*, 4026–4038.

Ingrin, J., and H. Skogby (2000), Hydrogen in nominally anhydrous upper-mantle minerals: Concentration levels and implications, *Eur. J. Mineral.*, *12*, 543–570.

Jaoul, O., and P. Raterron (1994), High-temperature deformation of diopside crystal: 3. Influence of PO_2 and SiO_2 precipitation, *J. Geophys. Res.*, *99*, 9423–9439.

Ji, S., and B. Xia (2002), *Rheology of Polyphase Earth Materials*, pp. 1–39, Polytechnic, New York.

Johnson, E. A., and G. R. Rossman (2003), The concentration and speciation of hydrogen in feldspars using FTIR and ^{1}H MAS NMR spectroscopy, *Am. Mineral.*, *88*, 901–911.

Johnson, E. A., and G. R. Rossman (2004), A survey of hydrous species and concentrations in igneous feldspars, *Am. Mineral.*, *89*, 586–600.

Katayama, I., and S. Nakashima (2003), Hydroxyl in clinopyroxene from the deep subducted crust: Evidence for H_2O transport into the mantle, *Am. Mineral.*, *88*, 229–234.

Kempton, P. D., H. Downes, L. A. Neymark, J. A. Wartho, R. E. Zartman, and E. V. Sharkov (2001), Garnet granulite xenoliths from the northern Baltic Shield: The underplated lower crust of a Palaeoproterozoic large igneous province?, *J. Petrol.*, *42*(4), 731–763.

Kohlstedt, D. L., H. Keppler, and D. C. Rubie (1996), Solubility of water in the α, β and γ phases of $(Mg, Fe)_2SiO_4$, *Contrib. Mineral. Petrol.*, *123*, 345–357.

Kröger, F. A., and H. J. Vink (1956), Relations between the concentrations of imperfections in crystalline solids, in *Solid State Physics 3*, edited by F. Seitz and D. Turnball, p. 367, Elsevier, New York.

Labusch, R., and W. Schroter (1980), Electrical properties of dislocations in semi-conductors, in *Dislocations in Solids*, edited by F. R. N. Nabarro, pp. 127–191, Elsevier, New York.

Mackwell, S. J., and D. L. Kohlstedt (1990), Diffusion of hydrogen in olivine: Implications for water in mantle, *J. Geophys. Res.*, *95*, 5079–5088.

Mackwell, S. J., M. E. Zimmerman, and D. L. Kohlstedt (1998), High-temperature deformation of dry diabase with application to tectonics on Venus, *J. Geophys. Res.*, *103*, 975–984.

Mclaren, A. C., R. F. Cook, S. T. Hyde, and R. C. Tobin (1983), The mechanisms of the formation and growth of water bubbles and associated dislocation loops in synthetic quartz, *Phys. Chem. Miner.*, *9*, 79–94.

Mei, S., and D. L. Kohlstedt (2000a), Influence of water on plastic deformation of olivine aggregates: 1. Diffusion creep regime, *J. Geophys. Res.*, *105*, 21,457–21,469.

Mei, S., and D. L. Kohlstedt (2000b), Influence of water on plastic deformation of olivine aggregates: 2. Dislocation creep regime, *J. Geophys. Res.*, *105*, 21,471–21,481.

Montanini, A., and R. Tribuzio (2001), Gabbro-derived granulite from the northern Apennines (Italy): Evidence for lower-crustal emplacement of tholeiitic liquids in post-Variscan times, *J. Petrol.*, *42*(12), 2259–2277.

Orowan, E. (1940), Problems of plastic gliding, *Proc. Phys. Soc.*, *52*, 8–22.

Paterson, M. S. (1969), The ductility of rocks, in *Physics of Strength and Plasticity*, edited by A. S. Argon, pp. 377–392, MIT Press, Cambridge, Mass.

Paterson, M. S. (1982), The determination of hydroxyl by infrared absorption in quartz silicate glasses and similar materials, *Bull. Mineral.*, *105*, 20–29.

Paterson, M. S. (1990), Rock deformation experimentation, in *The Brittle-Ductile Transition in Rocks*, *Geophys. Monogr. Ser.*, vol. 56, edited by A. G. Duba et al., pp. 187–194, AGU, Washington, D. C.

Poirier, J.-P. (1985), *Creep of Crystals: High-temperature Deformation Processes in Metals, Ceramics and Minerals*, 109 pp., Cambridge Univ. Press, New York.

Rybacki, E., and G. Dresen (2000), Dislocation and diffusion creep of synthetic anorthite aggregates, *J. Geophys. Res.*, *105*, 26,017–26,036.

Ryerson, F. J., and K. D. Mckeegan (1994), Determination of oxygen self-diffusion in akermanite, anorthite, diopside, and spinel: Implications for oxygen isotopic anomalies and the thermal histories of Ca-Al-rich inclusions, *Geochim. Cosmochim. Acta*, *58*, 3713–3734.

Shelton, G. L., and J. Tullis (1981), Experimental flow laws for crustal rocks, *Eos Trans. AGU*, *62*, 396.

Skogby, H. (1994), OH incorporation in synthetic clinopyroxene, *Am. Mineral.*, *79*, 240–249.

Skogby, H., and G. R. Rossman (1989), OH in pyroxene: An experimental study of incorporation mechanisms and stability, *Am. Mineral.*, *74*, 1059–1069.

Skogby, H., D. R. Bell, and G. R. Rossman (1990), Hydroxide in pyroxene: Variations in the natural environment, *Am. Mineral.*, *18*, 64–68.

Smyth, J. R., D. R. Bell, and G. R. Rossman (1991), Incorporation of hydroxyl in upper-mantle clinopyroxenes, *Nature*, *351*, 732–735.

Tullis, T. E., F. G. Horowitz, and J. Tullis (1991), Flow laws of polyphase aggregates from end-member flow laws, *J. Geophys. Res.*, *96*, 8081–8096.

Upton, B. G. J., P. Aspen, and R. W. Hinton (2001), Pyroxene and granulite xenoliths from beneath the Scottish Northern highlands terrane: Evidence for lower-crust/upper mantle relationships, *Contrib. Mineral. Petrol.*, *142*, 178–197.

Weertman, J. (1999), Microstructural mechanisms in creep, in *Mechanics and Materials: Fundamentals and Linkages*, edited by M. A. Meyers, R. W. Armstrong, and H. Kirchner, pp. 451–488, John Wiley, Hoboken, N. J.

Zimmerman, M. E., and D. L. Kohlstedt (2004), Rheological properties of partially molten lherzolite, *J. Petrol.*, *45*(N2), 275–298.

S. Chen, T. Hiraga, and D. L. Kohlstedt, Department of Geology and Geophysics, University of Minnesota, 310 Pillsbury Drive SE, Minneapolis, MN 55455, USA. (chen0705@umn.edu)